# Communications_____

## Comparison of the Physical Optics and Small Slope Theories for Polarimetric Thermal Emission From the Sea Surface

Joel T. Johnson

*Abstract*—**A comparison of the physical optics and small slope theories of emission from the sea surface is described. It is shown that the two theories produce identical results for "long wave" contributions to sea emission azimuthal variations up to third order in long wave surface slope when shadowing effects are neglected.**

*Index Terms*—**Passive remote sensing, radiometry, rough surface scattering, thermal emission.**

## I. INTRODUCTION

Recent experimental and theoretical studies have demonstrated the utility of polarimetric techniques in microwave passive remote sensing of ocean wind speed and direction [1]–[3]. The success of these studies has resulted in plans for a polarimetric radiometer to be included in the National Polar Orbiting Environmental Satellite System (NPOESS) series of satellites [4]. Analytical and numerical models for the calculation of ocean surface polarimetric thermal emission have also been developed, primarily through application of standard surface scattering approximate methods to calculate surface emissivity using Kirchhoff's law. Models based on the small perturbation method (SPM) [5], [6], a two-scale approach [7] and on the physical optics (PO) approximation [8] have been presented, as well as some limited numerical studies of short gravity/capillary wave emission with the method of moments [9]. Reference [10] has further revealed that use of the SPM for emission calculations results in a small slope, rather than small height, emission approximation, so that the SPM can provide accurate emission predictions even for surfaces with large heights in terms of the electromagnetic wavelength. Further studies with the SSA have been reported in [11]–[15].

Because the SSA captures emission contributions from sea surface waves with small slopes but arbitrary wavelengths relative to the electromagnetic wavelength $\lambda$, while PO theories should model emission contributions accurately only for sea wavelengths much greater than $\lambda$, a comparison of these theories for long wave contributions can provide information about both approximations. Particular attention in the comparison is given to the zeroth, first, second, and third azimuthal harmonic coefficients $T_\gamma^{(i)}$, $i = 0, 1, 2, 3$ for the four polarimetric brightness temperatures ($\gamma = h, v, U$ and $V$) as defined in [11].

## II. PHYSICAL OPTICS EMISSION THEORY

Several studies applying optical type theories to the prediction of emission from a rough surface at both microwave and optical frequencies have been reported [8], [16]–[24]. The work of [16] computes emissivity as one minus an integral over the upper hemisphere of standard rough surface far-field geometrical optics bistatic scattering coefficients. It is shown in [17] that this integration can be transformed into an integration over the surface slope probability density function (pdf); this form is reported by other authors [18]–[22]. Results of an identical form are also obtained by computing reflected powers directly on the surface with direct-plus-reflected surface currents [9], [23]. It should also be noted that the two-scale theory [7] reduces to an optical theory if the spectrum of short scale waves is set to zero.

The distinction between these references lies in the method used to treat shadowing and multiple scattering effects. Defining the $z$ direction as pointing from the mean surface plane into free space, the effects considered include

- incidence shadowing (local incident angle from radiometer to surface facet is greater than $90°$) [7], [8], [19]–[23]
- "Stogryn" shadowing (specular reflection of ray from radiometer to facet has a negative z component) [8], [16], [17], [21]–[24]
- "pdf scaling" (use of modified slope pdfs for approximate inclusion of shadowing effects) [20]–[23]
- multiple scattering contributions (Monte Carlo simulation up to third order) [8]

The relative importance of these effects generally increases both with the roughness of the surface and with the observation angle.

Emissivities can also be obtained by computing the total power transmitted into the sea medium; if power conservation is satisfied, results are identical to those computed from one minus the reflectivity. The shadowing effects above can be defined similarly and included when computing transmitted powers. However, [17] shows that optical emission theories do not conserve power if any shadowing effects are included and brightness temperatures become ambiguous. To avoid this problem, no shadowing or multiple scattering effects are included in the studies of this paper. However, it should be expected that the accuracy of optical emission models will degrade when any of the above shadowing or multiple scattering effects are significant.

The physical optics expression for the brightness temperature of a rough surface with physical temperature $T_s$ is then

$$
\begin{bmatrix} T_{Bh} \\ T_{Bv} \\ T_U \\ T_V \end{bmatrix} = T_s \left\langle \frac{-\left(\hat{n} \cdot \hat{k}_i\right)|\bar{n}|}{\cos\theta_i \left(1 - \left(\hat{n} \cdot \hat{k}_i\right)^2\right)} \right.
$$
$$
\left. \cdot \begin{bmatrix} \left(\hat{n} \cdot \hat{v}_i\right)^2 \left(1 - |R_h|^2\right) + \left(\hat{n} \cdot \hat{h}_i\right)^2 \left(1 - |R_v|^2\right) \\ \left(\hat{n} \cdot \hat{h}_i\right)^2 \left(1 - |R_h|^2\right) + \left(\hat{n} \cdot \hat{v}_i\right)^2 \left(1 - |R_v|^2\right) \\ 2\left(\hat{n} \cdot \hat{v}_i\right)\left(\hat{n} \cdot \hat{h}_i\right)\left(|R_v|^2 - |R_h|^2\right) \\ 0 \end{bmatrix} \right\rangle \quad (1)
$$

where $\theta_i$ is the radiometer incidence angle and

$$\hat{k}_i = \hat{x}\sin\theta_i - \hat{z}\cos\theta_i \quad (2)$$
$$\hat{h}_i = \hat{y} \quad (3)$$
$$\hat{v}_i = -\hat{x}\cos\theta_i - \hat{z}\sin\theta_i \quad (4)$$

are unit vectors along the radiometer look direction and in the horizontal and vertical polarization directions, respectively. The $\langle \cdot \rangle$ notation above refers to an average over the surface slope pdf, $f(\alpha, \beta)$, where $\alpha$ and $\beta$ are the surface slopes along and perpendicular to the

horizontal projection of the radiometer look direction, respectively. The upward pointing normal vector for a given surface "facet" is then

$$\hat{n} = \frac{1}{\sqrt{1 + \alpha^2 + \beta^2}} \left( \hat{z} - \hat{x}\alpha - \hat{y}\beta \right). \tag{5}$$

The Fresnel reflection coefficients $R_h$ and $R_v$ for a surface with complex relative permittivity $\epsilon$ are calculated at the local incidence angle $\theta_l$, determined from $\cos\theta_l = -\hat{n} \cdot \hat{k}_i$. Note there is no frequency dependence in (1) aside from variations in surface permittivity with frequency, as should be expected for an optical theory. The final PO brightness temperatures can be rewritten including the integration over the slope pdf as

$$T_\gamma = T_s \int_{-\infty}^{\infty} d\alpha \int_{-\infty}^{\infty} d\beta \, g_\gamma^{PO}(\alpha, \beta) f(\alpha, \beta) \tag{6}$$

where $g_\gamma^{PO}(\alpha, \beta)$ is defined as the product inside the ensemble average in (1) and remains a function of the radiometer observation angle and the surface permittivity.

## III. SMALL SLOPE APPROXIMATION

The small slope approximation expresses the change in flat surface brightness temperatures due to surface roughness as a series of terms in surface "quasislope" [10]. The first correction is at second order and the number of terms required in the series generally is expected to increase with both the surface slope and the observation angle. As described in [5], [10], and [11], the second-order small slope approximation expresses the change in flat surface brightness temperatures due to surface roughness effects as an integration over the surface directional spectrum $W(k_x, k_y)$

$$\Delta T_\gamma^{(2)} = -T_s \int dk_x \int dk_y \, W(k_x, k_y) \, g_\gamma^{(2)}(k_x, k_y) \tag{7}$$

where $g_\gamma^{(2)}$ is a "weighting function" obtained from the second-order SSA theory. To obtain emission contributions from surface waves with wavelengths much greater than $\lambda$, the weighting function can be expanded in a Taylor series about the origin

$$g_\gamma^{(2)}(k_x, k_y) \approx g_\gamma^{(2)}(0,0) + k_x g_{\gamma,k_x}^{(2)}(0,0) + k_y g_{\gamma,k_y}^{(2)}(0,0)$$
$$+ \frac{1}{2} k_x^2 g_{\gamma,k_x,k_x}^{(2)}(0,0) + k_x k_y g_{\gamma,k_x,k_y}^{(2)}(0,0)$$
$$+ \frac{1}{2} k_y^2 g_{\gamma,k_y,k_y}^{(2)}(0,0) + \cdots \tag{8}$$

where the additional subscripts indicate derivatives evaluated at the origin. The zeroth order term in this series is found to vanish and the first-order terms produce no emission contributions since the directional spectrum can have no first moments. Third and higher odd order terms also produce no contributions, while fourth and higher even order terms produce contributions which can be related to second moments involving higher derivatives of the surface. Second-order terms produce the dominant contributions, with results expressed in terms of surface slope variances and correlations:

$$\Delta T_\gamma^{(2)} \approx -T_s$$
$$\cdot \begin{bmatrix} \frac{1}{2} \left( g_{\gamma,k_x,k_x}^{(2)}(0,0)\langle S_x^2 \rangle + g_{\gamma,k_y,k_y}^{(2)}(0,0)\langle S_y^2 \rangle \right) \\ g_{\gamma,k_x,k_y}^{(2)}(0,0)\langle S_x S_y \rangle \end{bmatrix} \tag{9}$$

where the upper row applies for linear polarized brightnesses and the lower row for the correlation brightnesses; this separation is possible due to the weighting function symmetry properties discussed in [11]. For convenience, the quantities $\langle S_x^2 \rangle$ and $\langle S_y^2 \rangle$ are defined as the surface slope variances along or perpendicular to the radiometer look direction, respectively, so that weighting functions are evaluated with radiometer azimuth angle $\phi_i = 0$. If the surface up-wind and cross-wind slope variances are defined as $\langle S_u^2 \rangle$ and $\langle S_c^2 \rangle$, then for a radiometer observing at angle $\phi_i$ with respect to the up-wind direction:

$$\langle S_x^2 \rangle = \frac{1}{2} \left( \left[ \langle S_u^2 \rangle + \langle S_c^2 \rangle \right] + \left[ \langle S_u^2 \rangle - \langle S_c^2 \rangle \right] \cos 2\phi_i \right) \tag{10}$$

$$\langle S_x S_y \rangle = -\frac{1}{2} \left[ \langle S_u^2 \rangle - \langle S_c^2 \rangle \right] \sin 2\phi_i \tag{11}$$

$$\langle S_y^2 \rangle = \frac{1}{2} \left( \left[ \langle S_u^2 \rangle + \langle S_c^2 \rangle \right] - \left[ \langle S_u^2 \rangle - \langle S_c^2 \rangle \right] \cos 2\phi_i \right). \tag{12}$$

The azimuthal dependence of second order long wave emission contributions can then be explicitly written as

$$\Delta T_\gamma^{(2)} \approx -T_s \left( (\langle S_u^2 \rangle + \langle S_c^2 \rangle) \right.$$
$$\times \begin{bmatrix} \frac{1}{4} \left( g_{\gamma,k_x,k_x}^{(2)}(0,0) + g_{\gamma,k_y,k_y}^{(2)}(0,0) \right) \\ 0 \end{bmatrix}$$
$$+ (\langle S_u^2 \rangle - \langle S_c^2 \rangle)$$
$$\times \begin{bmatrix} \frac{1}{4} \left( g_{\gamma,k_x,k_x}^{(2)}(0,0) - g_{\gamma,k_y,k_y}^{(2)}(0,0) \right) \cos(2\phi_i) \\ -\frac{1}{2} g_{\gamma,k_x,k_y}^{(2)}(0,0) \sin(2\phi_i) \end{bmatrix} \right)$$
$$= -T_s \left( (\langle S_u^2 \rangle + \langle S_c^2 \rangle) \begin{bmatrix} h_{\gamma,0}(\theta_i,\epsilon) \\ 0 \end{bmatrix} \right.$$
$$\left. + (\langle S_u^2 \rangle - \langle S_c^2 \rangle) \begin{bmatrix} h_{\gamma,2}(\theta_i,\epsilon) \cos(2\phi_i) \\ h_{\gamma,2}(\theta_i,\epsilon) \sin(2\phi_i) \end{bmatrix} \right) \tag{13}$$

The $h_{\gamma,i}$ functions defined in the previous equations are the long wave functions of [11] and depend only on the incidence angle $\theta_i$ and the surface relative complex permittivity $\epsilon$. The index $i$ indicates the emission azimuthal harmonic obtained. Surface properties are completely described in the above limit by the up- and cross-wind slope variances alone, independent of the detailed functional form of the spectrum $W(k_x, k_y)$.

The third-order SSA [13]–[15] produces an additional correction for non-Gaussian random processes expressed in terms of an integral over the sea surface bispectrum $\Gamma(k_x, k_y, k_x', k_y')$ [15]

$$\Delta T_\gamma^{(3)} = -T_s \int dk_x \int dk_y \int dk_x'$$
$$\cdot \int dk_y' 2 \, \text{Re} \left\{ \Gamma\left(k_x, k_y, k_x', k_y'\right) g_\gamma^{(3)}\left(k_x, k_y, k_x', k_y'\right) \right\}. \tag{14}$$

Performing a similar Taylor expansion of the third-order weighting function and utilizing integral relationships between the bispectrum and third moments of surface slope [15] again produces a dominant contribution involving moments of the surface slope (see (15), shown at the bottom of the page). For a sea surface with only the $\langle S_u^3 \rangle$ and

$$\Delta T_\gamma^{(3)} \approx -T_s \begin{bmatrix} g_{\gamma,k_x,k_x,k_x'}^{(3)}(0,0,0,0) \langle S_x^3 \rangle + \left( g_{\gamma,k_y,k_y,k_x'}^{(3)}(0,0,0,0) + 2g_{\gamma,k_x,k_y,k_y'}^{(3)}(0,0,0,0) \right) \langle S_x S_y^2 \rangle \\ g_{\gamma,k_y,k_y,k_y'}^{(3)}(0,0,0,0) \langle S_y^3 \rangle + \left( g_{\gamma,k_x,k_x,k_y'}^{(3)}(0,0,0,0) + 2g_{\gamma,k_x,k_y,k_x'}^{(3)}(0,0,0,0) \right) \langle S_x^2 S_y \rangle \end{bmatrix} \tag{15}$$

$\langle S_u S_c^2 \rangle$ third moments (as in the sea surface slope pdf of [25]), these quantities are

$$\langle S_x^3 \rangle = \frac{3}{4} \left[ \langle S_u^3 \rangle + \langle S_u S_c^2 \rangle \right] \cos \phi_i$$
$$+ \frac{1}{4} \left[ \langle S_u^3 \rangle - 3 \langle S_u S_c^2 \rangle \right] \cos 3\phi_i \quad (16)$$

$$\langle S_x^2 S_y \rangle = -\frac{1}{4} \left[ \langle S_u^3 \rangle + \langle S_u S_c^2 \rangle \right] \sin \phi_i$$
$$-\frac{1}{4} \left[ \langle S_u^3 \rangle - 3 \langle S_u S_c^2 \rangle \right] \sin 3\phi_i \quad (17)$$

$$\langle S_x S_y^2 \rangle = \frac{1}{4} \left[ \langle S_u^3 \rangle + \langle S_u S_c^2 \rangle \right] \cos \phi_i$$
$$-\frac{1}{4} \left[ \langle S_u^3 \rangle - 3 \langle S_u S_c^2 \rangle \right] \cos 3\phi_i \quad (18)$$

$$\langle S_y^3 \rangle = -\frac{3}{4} \left[ \langle S_u^3 \rangle + \langle S_u S_c^2 \rangle \right] \sin \phi_i$$
$$+ \frac{1}{4} \left[ \langle S_u^3 \rangle - 3 \langle S_u S_c^2 \rangle \right] \sin 3\phi_i. \quad (19)$$

The azimuthal dependence of third order long wave contributions can then be explicitly written as shown in (20)–(21) at the bottom of the page, where $S_1^3 = \langle S_u^3 \rangle + \langle S_u S_c^2 \rangle$, $S_2^3 = \langle S_u^3 \rangle - 3\langle S_u S_c^2 \rangle$ and the derivatives are evaluated at $(k_x, k_y, k_x', k_y') = (0,0,0,0)$. This expansion describes azimuthal variations more explicitly than the long wave expansion of [15], in which only the up/down wind difference of brightness temperatures was considered. Again long wave first and third azimuthal harmonics are described by the functions $h_{\gamma,1}$ and $h_{\gamma,3}$ which depend only on the incidence angle and the surface permittivity. Surface properties are described completely by the $S_1^3$ and $S_2^3$ quantities which are related to the slope third moments $\langle S_u^3 \rangle$ and $\langle S_u S_c^2 \rangle$ and which model surface horizontal skewness effects.

## IV. COMPARISON OF THEORIES

The form of the SSA results suggests that an expansion of the kernel of the PO integral in a slope power series

$$g_\gamma(\alpha, \beta)^{PO} \approx g_\gamma^{PO}(0,0) + \alpha g_{\gamma,\alpha}^{PO}(0,0) + \beta\, g_{\gamma,\beta}^{PO}(0,0)$$
$$+ \frac{1}{2}\alpha^2\, g_{\gamma,\alpha,\alpha}^{PO}(0,0) + \alpha\beta g_{\gamma,\alpha,\beta}^{PO}(0,0)$$
$$+ \frac{1}{2}\beta^2 g_{\gamma,\beta,\beta}^{PO}(0,0) + \frac{1}{6}\alpha^3 g_{\gamma,\alpha,\alpha,\alpha}^{PO}(0,0)$$
$$+ \frac{1}{2}\alpha^2 \beta g_{\gamma,\alpha,\alpha,\beta}^{PO}(0,0) + \frac{1}{2}\alpha\beta^2 g_{\gamma,\alpha,\beta,\beta}^{PO}(0,0)$$
$$+ \frac{1}{6}\beta^3 g_{\gamma,\beta,\beta,\beta}^{PO}(0,0) + \cdots \quad (22)$$

where the additional subscripts indicate derivatives evaluated at the origin, should generate a useful comparison. Such an expansion has been demonstrated for nonpolarimetric brightness temperatures in [10], [18], and [23]. The first term in the series produces the brightness temperature of a flat surface while higher order terms in the series produce corrections to the flat surface brightness temperature involving moments of the surface slope. Because the sea surface should have no average up-wind or cross-wind slopes, the first-order terms above are zero and the first contribution comes from the second-order terms

$$\Delta T_\gamma^{(2)} = T_s \left( \left[ \begin{array}{c} \frac{1}{2} \left( \langle S_x^2 \rangle g_{\gamma,\alpha,\alpha}^{PO}(0,0) + \langle S_y^2 \rangle g_{\gamma,\beta,\beta}^{PO}(0,0) \right) \\ \langle S_x S_y \rangle\ g_{\gamma,\alpha,\beta}^{PO}(0,0) \end{array} \right] \right). \quad (23)$$

The separation for the linear and correlation brightnesses occurs due to symmetry properties of the weighting functions. If the slope variances are again rewritten in terms of the up-wind and cross-wind slope variances, the azimuthal dependence becomes explicit

$$\Delta T_\gamma^{(2)} \approx T_s \left( \left( \langle S_u^2 \rangle + \langle S_c^2 \rangle \right) \left[ \begin{array}{c} \frac{1}{4} \left( g_{\gamma,\alpha,\alpha}^{PO}(0,0) + g_{\gamma,\beta,\beta}^{PO}(0,0) \right) \\ 0 \end{array} \right] \right.$$
$$+ \left( \langle S_u^2 \rangle - \langle S_c^2 \rangle \right)$$
$$\left. \cdot \left[ \begin{array}{c} \frac{1}{4} \left( g_{\gamma,\alpha,\alpha}^{PO}(0,0) - g_{\gamma,\beta,\beta}^{PO}(0,0) \right)\ \cos(2\phi_i) \\ -\frac{1}{2} g_{\gamma,\alpha,\beta}^{PO}(0,0)\ \sin(2\phi_i) \end{array} \right] \right)$$
$$= -T_s \left( \left( \langle S_u^2 \rangle + \langle S_c^2 \rangle \right) \left[ \begin{array}{c} h_{\gamma,0}^{PO}(\theta_i, \epsilon) \\ 0 \end{array} \right] \right.$$
$$+ \left( \langle S_u^2 \rangle - \langle S_c^2 \rangle \right)$$
$$\left. \cdot \left[ \begin{array}{cc} h_{\gamma,2}^{PO}(\theta_i, \epsilon) & \cos(2\phi_i) \\ h_{\gamma,2}^{PO}(\theta_i, \epsilon) & \sin(2\phi_i) \end{array} \right] \right). \quad (24)$$

Following similar steps, the final result for third-order contributions is shown in (25)–(26) at the bottom of the page.

Both the second-order [(13) and (24)] and third-order [(21) and (26)] SSA and PO theories obtain identical forms for long-wave contributions. Identical predictions will be obtained if the long wave functions $h_{\gamma,i}$ and $h_{\gamma,i}^{PO}$ are identical. While the complexity of these functions makes an analytical comparison difficult, the fact that the long wave functions depend only on observation angle and surface relative permittivity allows comparisons to be made through simple plots versus observation angle. Figs. 1–3 compare the long wave functions $h_{\gamma,i}(\theta_i, \epsilon)$ (lines) and $h_{\gamma,i}^{PO}(\theta_i, \epsilon)$ (symbols) for $i = 0$ to 3 in h, v and U polarizations, respectively, for a surface with relative permittivity $\epsilon = 29.04 + i35.55$ (approximate value for sea water at 19.35 GHz [26]). The curves illustrated show the long wave functions to be identical; differences between the curves plotted were within the precision

$$\Delta T_\gamma^{(3)} \approx -T_s \left( \left[ \begin{array}{c} \frac{1}{4} S_1^3 \left[ 3g_{\gamma,k_x,k_x,k_x'}^{(3)} + g_{\gamma,k_y,k_y,k_x'}^{(3)} + 2g_{\gamma,k_x,k_y,k_y'}^{(3)} \right] \cos(\phi_i) \\ -\frac{1}{4} S_1^3 \left[ 3g_{\gamma,k_y,k_y,k_y'}^{(3)} + g_{\gamma,k_x,k_x,k_y'}^{(3)} + 2g_{\gamma,k_x,k_y,k_x'}^{(3)} \right] \sin(\phi_i) \end{array} \right] \right.$$
$$\left. + \left[ \begin{array}{c} \frac{1}{4} S_2^3 \left[ g_{\gamma,k_x,k_x,k_x'}^{(3)} - g_{\gamma,k_y,k_y,k_x'}^{(3)} - 2g_{\gamma,k_x,k_y,k_y'}^{(3)} \right] \cos(3\phi_i) \\ \frac{1}{4} S_2^3 \left[ g_{\gamma,k_y,k_y,k_y'}^{(3)} - g_{\gamma,k_x,k_x,k_y'}^{(3)} - 2g_{\gamma,k_x,k_y,k_x'}^{(3)} \right] \sin(3\phi_i) \end{array} \right] \right) \quad (20)$$

$$\approx -T_s \left( S_1^3\, h_{\gamma,1}(\theta_i, \epsilon) \left[ \begin{array}{c} \cos(\phi_i) \\ \sin(\phi_i) \end{array} \right] + S_2^3\, h_{\gamma,3}(\theta_i, \epsilon) \left[ \begin{array}{c} \cos(3\phi_i) \\ \sin(3\phi_i) \end{array} \right] \right) \quad (21)$$

$$\Delta T_\gamma^{(3)} \approx T_s \left( \left[ \begin{array}{c} +\frac{1}{8} S_1^3 \left[ g_{\gamma,\alpha,\alpha,\alpha}^{PO} + g_{\gamma,\alpha,\beta,\beta}^{PO} \right] \cos(\phi_i) \\ -\frac{1}{8} S_1^3 \left[ g_{\gamma,\beta,\beta,\beta}^{PO} + g_{\gamma,\alpha,\alpha,\beta}^{PO} \right] \sin(\phi_i) \end{array} \right] \right.$$
$$\left. + \left[ \begin{array}{c} \frac{1}{24} S_2^3 \left[ g_{\gamma,\alpha,\alpha,\alpha}^{PO} - 3g_{\gamma,\alpha,\beta,\beta}^{PO} \right] \cos(3\phi_i) \\ \frac{1}{24} S_2^3 \left[ g_{\gamma,\beta,\beta,\beta}^{PO} - 3g_{\gamma,\alpha,\alpha,\beta}^{PO} \right] \sin(3\phi_i) \end{array} \right] \right) \quad (25)$$

$$= -T_s \left( S_1^3\, h_{\gamma,1}^{PO}(\theta_i, \epsilon) \left[ \begin{array}{c} \cos(\phi_i) \\ \sin(\phi_i) \end{array} \right] + S_2^3\, h_{\gamma,3}^{PO}(\theta_i, \epsilon) \left[ \begin{array}{c} \cos(3\phi_i) \\ \sin(3\phi_i) \end{array} \right] \right) \quad (26)$$
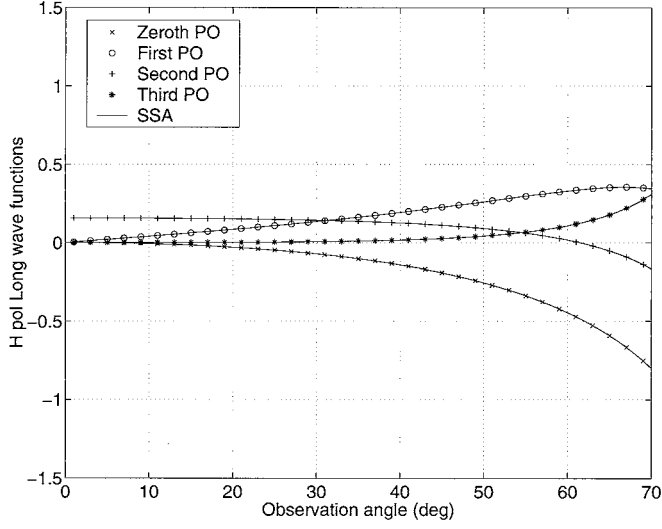
Fig. 1. Horizontal polarization long wave functions $h_{\gamma,i}(\theta_i, \epsilon)$ and $h_{\gamma,i}^{PO}(\theta_i, \epsilon)$.
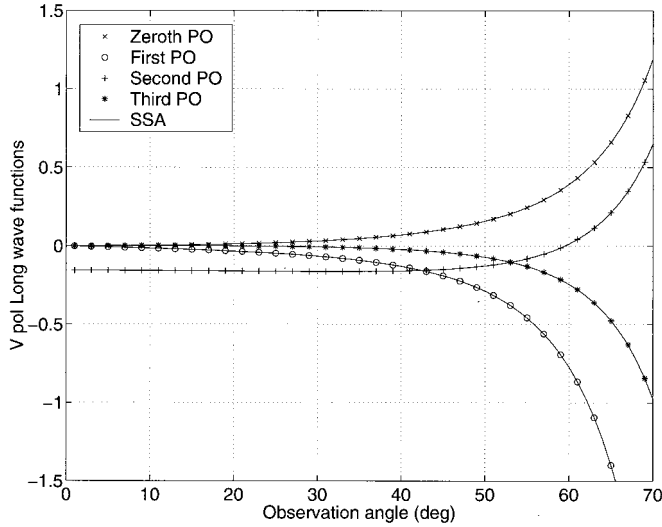


Fig. 2. Vertical polarization long wave functions $h_{\gamma,i}(\theta_i, \epsilon)$ and $h_{\gamma,i}^{PO}(\theta_i, \epsilon)$.



Fig. 3. $U$ polarization long wave functions $h_{\gamma,i}(\theta_i, \epsilon)$ and $h_{\gamma,i}^{PO}(\theta_i, \epsilon)$.

for a given polarization will depend on relationships between slope moments; results illustrating long-wave contributions for given sea spectral models are provided in [15].

## V. CONCLUSIONS

The results of this paper confirm that the small slope and physical optics emission theories produce identical predictions up to third order in surface slope for long wave contributions to emission azimuthal harmonics when shadowing and multiple scattering effects are neglected in the physical optics calculations. This conclusion is independent of the surface spectral model used in the small slope theory and the surface slope probability density function used in the optical theory. Since the two-scale theory also obtains long wave contributions from an optical theory, all current theories are in agreement on the basic form for these contributions. It is not unreasonable to expect that SSA theories to fourth or higher order in surface slope could continue to match the physical optics theory for long wave contributions; such agreement would suggest that the PO method without shadowing should be applied to compute long wave contributions when shadowing and multiple scattering effects are not significant. However, the higher even order terms from the second order SSA expansion in (8) will capture contributions from surface curvature and higher order derivative moments that are not included in the PO theory; the distinction between knowledge of the directional spectrum of a random process versus knowledge of the single point slope probability density function clarifies that the PO theory is a local approximation only, while the SSA includes some nonlocal effects. The SSA theory also can include contributions from surface features on the order of or shorter than the electromagnetic wavelength when the complete SSA integral expressions are applied and can potentially capture shadowing and multiple scattering contributions accurately if a sufficient number of terms in the SSA series is used.

of the calculations. No fourth Stokes' parameter curves are illustrated, as both theories predict long wave contributions to this term to be negligible. Similar agreement is obtained with other values of the surface relative permittivity.

Figs. 1–3 show the relative importance of long wave contributions to differing azimuthal harmonics to vary according to the polarization and incidence angle considered. Emission brightness temperature harmonics are obtained simply by multiplying the long wave functions of the figures by $-T_s \tilde{S}^2$ and $-T_s \tilde{S}^3$ for even and odd harmonics, respectively, where $\tilde{S}^2$ and $\tilde{S}^3$ are appropriate slope moments as defined as in (24) and (26). The variation of these harmonics versus observation angle is therefore independent of surface properties and captured by the curves illustrated. First harmonic long wave functions are seen to be less significant in horizontal polarization than in the other polarizations. Odd harmonic long wave functions show a general increasing trend in amplitude with the observation angle (with the exception of the first harmonic for horizontal polarization), while second harmonic long wave functions show a zero crossing as the observation angle increases. Relationships between the amplitudes of emission harmonics
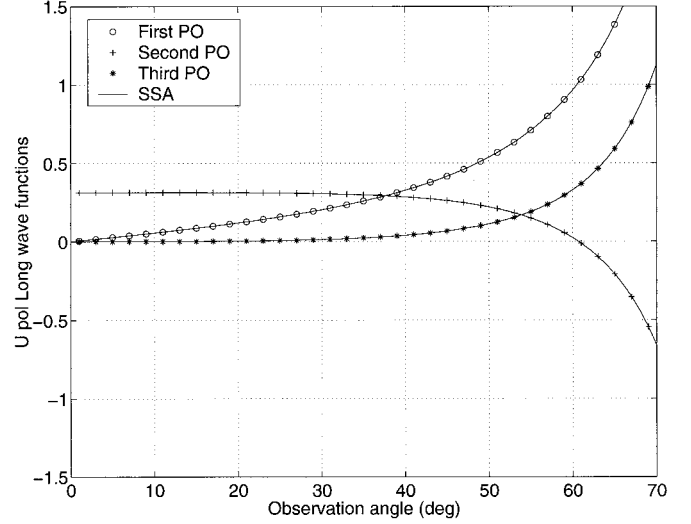
## REFERENCES

[1] M. S. Dzura, V. S. Etkin, A. S. Khrupin, M. N. Pospelov, and M. D. Raev, "Radiometers polarimeters: Principles of design and applications for sea surface microwave emission polarimetry," in *Proc. IGARSS Conf.*, 1992, pp. 1432–1434.

[2] S. H. Yueh, W. J. Wilson, F. K. Li, S. V. Nghiem, and W. B. Ricketts, "Polarimetric measurements of sea surface brightness temperatures using an aircraft K-band radiometer," *IEEE Trans. Geosci. Remote Sensing*, vol. 33, pp. 85–92, Jan. 1995.

[3] J. R. Piepmeier and A. J. Gasiewski, "High-resolution passive polarimetric microwave mapping of ocean surface wind vector fields," *IEEE Trans. Geosci. Remote Sensing*, vol. 39, pp. 606–622, Mar. 2001.

[4] S. D. Gasster and G. M. Flaming, "Overview of the conical microwave imager/sounder development for the NPOESS program," in *Proc. IGARSS Conf.*, vol. 1, 1998, pp. 268–271.

[5] V. G. Irisov, I. G. Trokhimovskii, and V. S. Etkin, "Radiothermal spectroscopy of the sea-surface," *Dokl. Akad. Nauk SSSR*, vol. 297, pp. 587–589, 1987.

[6] S. H Yueh, R. Kwok, F. K. Li, S. V. Nghiem, and W. J. Wilson, "Polarimetric passive remote sensing of ocean wind vectors," *Radio Sci.*, vol. 29, pp. 799–814, 1994.

[7] S. H. Yueh, "Modeling of wind direction signals in polarimetric sea surface brightness temperatures," *IEEE Trans. Geosci. Remote Sensing*, vol. 35, pp. 1400–1418, Nov. 1997.

[8] D. B. Kunkee and A. J. Gasiewski, "Simulation of passive microwave wind direction signatures over the ocean using an asymmetric-wave geometrical optics model," *Radio Sci.*, vol. 32, p. 59, 1997.

[9] J. T. Johnson, R. T. Shin, L. Tsang, K. Pak, and J. A. Kong, "A numerical study of ocean polarimetric thermal emission," *IEEE Trans. Geosci. Remote Sensing*, vol. 37, pp. 8–20, Jan. 1999.

[10] V. G. Irisov, "Small-slope expansion for thermal and reflected radiation from a rough surface," *Waves in Random Media*, vol. 7, pp. 1–10, 1997.

[11] J. T. Johnson and M. Zhang, "Theoretical study of the small slope approximation for ocean polarimetric thermal emission," *IEEE Trans. Geosci. Remote Sensing*, vol. 37, pp. 2305–2316, Sept. 1999.

[12] M. Zhang and J. T. Johnson, "Comparison of modeled and measured second azimuthal harmonics of ocean surface brightness temperatures," *IEEE Trans. Geosci. Remote Sensing*, vol. 39, pp. 448–452, Feb. 2001.

[13] V. G. Irisov, "Azimuthal variations of the microwave radiation from a slightly non-Gaussian sea surface," *Radio Sci.*, vol. 53, pp. 65–82, 2000.

[14] Y. G. Trokhimovskii and V. G. Irisov, "The analysis of wind exponents retrieved from microwave radar and radiometric measurements," *IEEE Trans. Geosci. Remote Sensing*, vol. 38, pp. 470–479, Jan. 2000.

[15] J. T. Johnson and Y. Cai, "A theoretical study of sea surface up/down wind brightness temperature differences," *IEEE Trans. Geosci. Remote Sensing*, vol. 40, pp. 66–78, Jan. 2002.

[16] A. Stogryn, "The apparent temperature of the sea at microwave frequencies," *IEEE Trans. Antennas Propagat.*, vol. 15, pp. 278–286, 1967.

[17] L. Tsang and J. A. Kong, "Energy conservation for reflectivity and transmissivity at a very rough surface," *J. Appl. Phys.*, vol. 51, pp. 673–680, 1980.

[18] ——, "Asymptotic solution for the reflectivity of a very rough surface," *J. Appl. Phys.*, vol. 51, pp. 681–690, 1980.

[19] L. Tsang, J. A. Kong, and R. T. Shin, *Theory of Microwave Remote Sensing*. New York: Wiley, 1985.

[20] Y. Yoshimori, K. Itoh, and Y. Ichioka, "Thermal radiative and reflective characteristics of a wind-roughened water surface," *J. Opt. Soc. Amer. A.*, vol. 11, pp. 1886–1893, 1994.

[21] D. E. Freund, R. I. Joseph, D. J. Donohue, and K. T. Constantikes, "Numerical computations of rough sea surface emissivity using the interaction probability density," *J. Opt. Soc. Amer. A.*, vol. 14, pp. 1836–1849, 1997.

[22] C. Bourlier, G. Berginc, and J. Saillard, "Theoretical study on two-dimensional gaussian rough sea surface emission and reflection in the infrared frequencies with shadowing effect," *IEEE Trans. Geosci. Remote Sensing*, vol. 39, pp. 379–392, Feb. 2001.

[23] D. V. Mikhailova and I. M. Fuks, "Emissivity of a statistically rough surface including multiple reflections," *Sov. J. Commun. Technol. Elect.*, vol. 38, pp. 128–136, 1993.

[24] A. Camps, I. Corbella, and J. M. Rius, "Extension of Kirchhoff method under stationary phase approximation to determination of polarimetric thermal emission from the sea," *Electron. Lett.*, vol. 34, pp. 1501–1503, 1998.

[25] C. Cox and W. Munk, "Measurement of the roughness of the sea surface from photographs of the sun's glitter," *J. Opt. Soc. Amer.*, vol. 44, pp. 838–850, 1954.

[26] L. A. Klein and C. T. Swift, "An improved model for the dielectric constant of sea water at microwave frequencies," *IEEE Trans. Antennas Propagat.*, vol. AP-25, pp. 104–111, Jan. 1977.